

## VIBRATION ANALYSIS OF PROSTHETIC KNEES IMPLANT USING FEM APPROACH

Yogesh Sanjay Pathare<sup>1</sup>, Dr. Manish R Billore<sup>2</sup>

<sup>1</sup>Mechanical Engineering, Research Scholar, Oriental University, Gate No.1, Sanwer Road, Opposite Revati Range, Jakhya, Indore, Madhya Pradesh – 453555 Indore, India

<sup>2</sup> Research Supervisor, Mechanical Engineering, , Oriental University, Gate No.1, Sanwer Road, Opposite Revati Range, Jakhya, Indore, Madhya Pradesh – 453555 Indore, India

### ABSTRACT

In this study, a vibration analysis of prosthetic knee implants was conducted using the finite element approach. This causes pain in the knee joint, which finally necessitates the urgent installation of prosthetic components. The objective of this study was to assess tibial section depth and the effect of body weight on tibial bearing pressure. Utilizing Ansys Workbench, do an analysis on average-weight patients and obese patients, while applying observations. This is performed alongside an equal weight. Using ANSYS, investigate the impacts of Human Frequency on a range of Materials and Shapes. Since more than forty years, finite element analysis has been used to research and evaluate mechanical behavior of complete joint replacements. Incorporating finite elements into the procedure of designing, developing, & pre-clinical evaluating complete joint replacements was becoming increasingly prevalent. Therefore in this work Static structural and Modal analysis is done in ANSYS and finally comparative results are found out as concluding part.

**Keywords:** Vibration, Vibration analysis, joint, Prosthetic Knees, knee cap, knee joint, FEM Approach and Vibration Analysis of Prosthetic Knees.

### 1. INTRODUCTION

The knee joint in humans is a weight-bearing synovial diarthrosis complex joint. Knee consists of femur, tibia, fibula, & patella. In addition to bending and straightening, there is a tiny rotating component to the knee's movement. Quadriceps & hamstrings are muscles of knee that cross the knee joint. The quadriceps are located at front of knee, while the hamstrings are located in the rear. Equally vital in the knee joint are the ligaments, which keep the joint together. In summary, the bones support the knee & give the joint's solid structure, the muscles work the joint, as well as the ligaments stabilize it.

As a numerical method approach, analysis of finite elements has been used to tackle several engineering issues. This method has been applied in biomedical engineering to evaluate prosthetic bone joints. Pressures at contact area, the heat flow and temperature gradient at the contact zone, and the varied biomaterials for the prostheses are relevant for forecasting the risk of knee prosthesis component injury. This has sparked the interest of biomaterials studygroup in determining stresses inside tibial implant., studying the distribution of heat, and investigating biomaterials. In this context, several computer analyses on the mechanics of the natural and artificial knees have been undertaken. There is presented findings on stress distribution using 2-dimensional dynamic models of knee. Stress may be predicted by both two and three knee models. To forecast the contact mechanics under dynamic loading, an explicit dynamic models

were developed. During articulation of whole knee systems, friction creates surface heat, resulting in damage and failure. In literature, however, little is known about interface assessment of prosthetic femoral/tibial joints for various material combinations and heat analysis. In light of the aforementioned, this research aims to quantify contact stresses and perform a thermal investigation of the femoral/tibia joint for various composite material.

**Knee Joint**

In the past, prosthetic knee joints have generated considerable attention. Different researchers have been working on the prosthetic knee joint throughout time in an effort to solve difficulties such as geometric modeling, stress assessment among the articular surfaces, reliability & fatigue life, wear, and dynamic analysis, among others. A joint is the point of contact between two or more bones. 360 joints make up the human body. They are designed to enable mobility (with the exception of the skull) and give mechanical support. Joints in the human body are primarily classed structurally and functionally, as seen in Figure. Functional classification is established by the degree of mobility between articulating bones, while structural classification is based by how the bones link to one another. In actuality, there is substantial crossover among the two categorization categories.

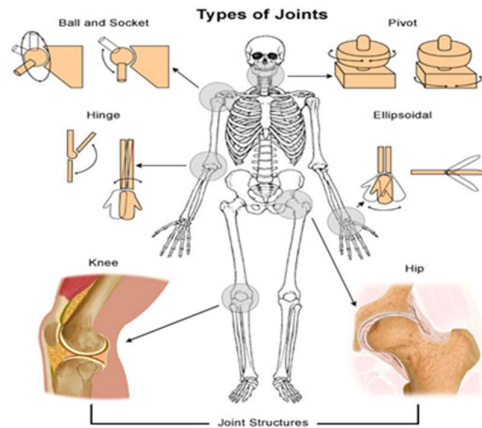


**Fig.1.1 Joints in the human body**

**Knee joint replacement**

Knee arthroplasty, often known as a knee replacement, is a surgical surgery that replaces the knee's weight-bearing surfaces to alleviate pain and impairment. Common indications for the procedure include osteoarthritis. There are two main types of knee replacement surgery: partial and complete. In most cases, metal and plastic components are used to recreate the natural form of the knee joint & restore mobility after knee's cartilage and joint surfaces have been removed due to illness or injury.



**Fig.1.2 knee Prostheses**

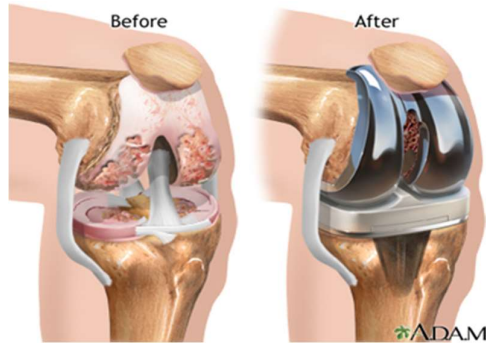


**Fig.1.4 Knee joint replacement**

Knee replacement surgery is the removal of damaged cartilage and bone from the knee joint. After that, a knee prosthesis constructed of synthetic materials is inserted. It's possible to implant these components on any of the knee's three articular surfaces: Part of the thigh bone that sits lower than the knee. The femur is the name for this leg bone. The top portion of the shin bone, the largest bone in the lower leg. The tibia is the name for this leg bone.

Usually, femur and tibia are the two prosthetic components, which are used to replace the affected knee. Fig shows the knee prostheses. The upper part is the femur and the lower part is the tibia. Fig shows the femorotibial joint in which the femur component (metal surface) is fixed to femur bone and tibia insert (plastic surface) is fixed to tibia bone. The femur is made of metal or alloy and tibia is made of plastic. These materials are called biomaterials which have to be biocompatible.

## 2. LITERATURE REVIEW

For the research of literature review there are papers which are selected belonging to journals. Papers which are selected from 2010 to 2021. Literature review belonging to Vibration Analysis of Prosthetic Knees Implant Using FEM Approach.

**Ayad M. Takhakh (2018)** study of Prosthetic Foot Manufacturing and Analysis for Pirogoff Amputees. This work uses a vacuum pressure technique to build a partial foot prosthesis socket out of three different kinds of laminated composite materials to test its tensile and fatigue capabilities. Lamination 80:20 served as the composite material matrix, and nine other lamination types were used to strengthen it (perlon, fiber glass and carbon). These experiments revealed that the mechanical characteristics of perlon were as follows:  $y=33.8\text{Mpa}$ ,  $ult=35.6\text{Mpa}$ , and  $E=1.037\text{GPa}$ . Three layers of material were tested, and the results were  $y=55\text{Mpa}$ ,  $ult=55.4\text{Mpa}$ , and  $E=1.57\text{GPa}$ . The results of the tests conducted on the (hybrid CF-GF) layers were  $y=112\text{Mpa}$ ,  $ult=150\text{Mpa}$ , and  $E=1.66\text{GPa}$ . High pressure readings of (112Kpa) and (108Kpa) were reported for the lateral and posterior parts of the prosthetic socket during the determination of internal pressure utilizing the (F-socket) Mat scan sensor. Layers of composite material (3Perlon+3fiberglass+3perlon) and hybrid CF-GF layers both have safety factors of about (1.146) and are therefore suitable for use in design.

**M. Woiczinski (2016)** The treatment for osteoarthritis of the knee is (TKA). However, postoperative discomfort is experienced by a significant minority of individuals (19%). A knee rig's boundary conditions served as the inspiration for a finite element model. A whole knee prosthesis was implanted without patella resurfacing after a 3D model of the patient's leg was created using MRI scan data. The computational model of the patellofemoral and femorotibial joint was validated using experimental data from a knee rig. The performed finite element

model produces results that are consistent with the experimental findings. As a result, the finite element model developed for this investigation might be used in future clinical studies to get a more thorough understanding of the clinical features after TKA with an unresurfaced patella.

**Keziah Cook (2020)** investigated the cost-effectiveness of a gene therapy for treating hemophilia A. Hemophilia A is a coagulation factor VIII (FVIII) deficiency/defective illness that causes an increased risk of spontaneous bleeding episodes, which may eventually damage joints and cause persistent discomfort. Prophylactic FVIII is used to treat most severe cases of hemophilia A, but it is expensive, must be infused often, and must be taken for the rest of the patient's life. For the treatment of severe hemophilia A, researchers are working on a gene therapy called valoctocogene roxaparvovec. The cost-effectiveness of valoctocogene roxaparvovec therapy compared to preventative treatment was analyzed using this model.

**Elena Losina, PhD (2016)** was studied, Cost-Effectiveness of Diet & Exercise for Patients with Obesity-Related Knee Osteoarthritis Patients with knee osteoarthritis (OA) lost an average of 10.6 kilograms (23 pounds) and saw a decrease in pain of 51 percent after participating in an intense diet and exercise (D+E) program, according to the Intensive Diet and Exercise for Arthritis (IDEA) study. We looked at how much it would cost to include this D+E program in the treatment of individuals with knee OA who were overweight or obese (body mass index  $\geq 27$  kg/m<sup>2</sup>). The Osteoarthritis Policy Model was used to calculate the quality-adjusted life-years (QALYs) gained and the lifetime expenses incurred by patients with knee OA who were overweight or obese with and without the D+E program. The incremental cost-effectiveness ratio (ICER) was used to compare treatment options in terms of their relative efficacy and cost-effectiveness. The author looked at a range of cost-effectiveness ratios, from \$50,000 to \$100,000 to \$200,000 every (QALY). We analyzed data from the healthcare industry and the larger society throughout the course of a lifetime. The yearly discount rate for both costs and QALYs was 3%. The IDEA study served as a basis for the development of D+E features. Parameter uncertainty and the impact of extending the D+E program length were assessed using deterministic and probabilistic sensitivity analysis (PSA)..

**Bart S Ferket (2017)** Resulting financial effects of widespread total knee replacement procedures The study analyzed data from the Osteoarthritis Initiative. The purpose of this research is twofold: (1) to evaluate how total knee replacement improves quality of life for patients with knee osteoarthritis; and (2) to determine differences in lifetime costs and quality adjusted life years (QALYs) associated with use according to symptom severity. Replication among patients with knee osteoarthritis in the MOST cohort confirmed the findings, which were robust in the face of multiple alternative scenarios, such as higher rates of total knee replacement and mortality and the inclusion of non-healthcare costs, while remaining sensitive to higher rates of quality of life decline in the absence of surgery. For patients with SF-12 PCS scores of 40, total knee replacement becomes financially viable if the cost of hospitalization is less than \$14,000. This is based on the cost effectiveness criteria of \$200000/QALY.

### 3. METHODOLOGY

The articulating bony components of a human knee are a complex system. These structures are subjected to significant stresses and relative displacements as a result of the many activities that make up a typical day. Studies based on finite element models have been acknowledged and relied upon for a long time as trustworthy supplementary instruments in the investigation of human articulations. The accurate control of loads, motion, boundary conditions, and

structural modifications that can be achieved via such numerical studies is an advantage they may be used to great effect in parametric analyses of joint response. Output data from these sorts of model studies, such as ligament forces, contact forces/areas, and cartilage stresses, are quite valuable. In the examination of Total knee failure, the use of finite element techniques has seen widespread use.

### **3.1. Problem statement of the study**

4. For four decades, finite component has been used in mechanical total joint replacements. Complete joint substitutions will be employed in the creative, output, and pre-clinical research processes. To be appropriate, simulations must take a number of co approach that includes real-world considerations, be holistic and thus supported by data, and have a greater degree of corroborating evidence. ANSYS is the Girly examination of something like the joint when the knee is straight. With various combinations of analyses, biomaterial analysis can produce varying results. If the CATIA modelling is complete, the file will be shipped into ANYS and entwined into finite elements, or finite dampers, before the solid model is divided up into smaller units known as Content Property Dividing.

#### **Aim of the study:**

“Vibration Analysis of Prosthetic Knees Implant Using FEM Approach”

### **4.1. Objectives of the study**

1. To study different type of knees implant case study and its material and methods used for various cases from hospital patient data.
2. To calculate the lifetime cost-effectiveness of knee implant of three materials used in operations.
3. To analyse body mass patients and use them in combination with a similar importance to be used with obese people, as well as to implement observational data in Ansys Workbench and vibration analysis in ANSYS WORKBENCH.
4. To perform experimental results and comparison on 3 biometric materials Cobalt Chromium , titanium alloy (Ti6Al4V), and nickel titanium (NiTi).are the biomaterials under consideration for knees implant.

### **4.2. Schematic work plan**

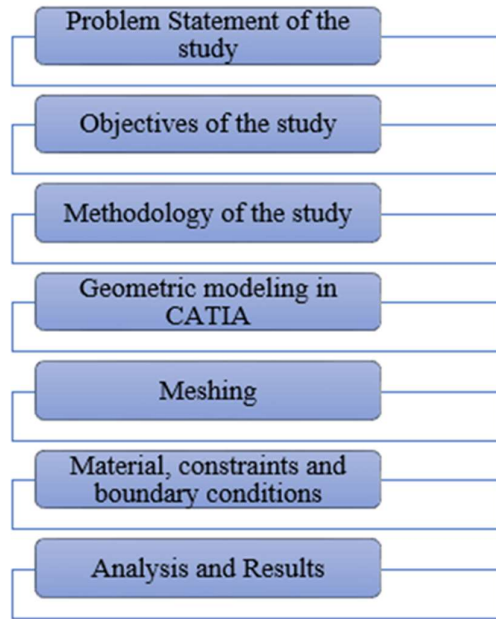


Fig.3.1 Shows the schematic work plan

**4.3. Material Properties of selected materials**

The different biomaterials considered for knees are Cobalt-Chromium (CoCr), titanium alloy (Ti6Al4V) and Nickel titanium (NiTi). These three materials has good biocompatibility with human body system.

**Table.3.1 Material Properties of Cobalt-Chromium (CoCr)**

Properties	Values
Compound Formula	CoCr
Molecular Weight	110.93
Density	10 g/cm <sup>3</sup>
Electrical Resistivity	-6 10x Ω-m
Poisson's Ratio	0.29
Tensile Strength	1130 to 1900 MPa (Ultimate)/ 470 to 1600 MPa (Yield)
Thermal Conductivity	9.4 W/m-K
Thermal Expansion	12 μm/m-K
Young's Modulus	210 GPa

**Table.3.2 Material Properties of Titanium Alloy (Ti-6Al-4V)**

Properties	Values
Compound Formula	Ti-6Al-4V
Density	4.429 Mg/cm <sup>3</sup>
Resistivity	168 x 10 <sup>-8</sup> Ω-m
Poisson's Ratio	0.31
Tensile Strength	862 to 1200 MPa
Thermal Conductivity	7.1 W/m-K
Thermal Expansion	8.7 μm/m-K
Young's Modulus	110 GPa

**Table.3.3 Material Properties of Ni-Ti Alloy (NiTi)**

Properties	Values
Compound Formula	NiTi
Density	6.45 g/cm <sup>3</sup>

Resistivity	$82 \times 10^{-6} \Omega\text{-cm}$
Poisson's Ratio	0.33
Tensile Strength	1900 MPa
Thermal Conductivity	0.18 W/m-K
Thermal Expansion	$11 \times 10^{-6}/^{\circ}\text{C}$
Young's Modulus	75–83 GPa

#### 4. EXPERIMENTAL RESULTS

##### 5. Universal Testing Machine (UTM)

Testing the tensile & compressive strength of materials requires a universal testing machine (UTM), also known as a universal tester, materials testing machine, or materials test frame. Older terminology for tensile testing machines is "tensometer.". It can conduct several typical tensile & compression tests on a variety of materials, components, & structures (i.e., it is versatile).



Fig.4.3. Universal Testing Machine

##### 6. Hardness test

The medical device and electronics sectors produce products that are fundamentally distinct from those of the traditional manufacturing sector. These high-technology goods with essential end-use applications are often significantly smaller and need tighter tolerances and higher material consistency. Their manufacturing materials must constantly exhibit the appropriate qualities to guarantee that the product design satisfies performance requirements.



Fig.4.4. Hardness Test Machine

##### 7. Work during Experimental Period



Fig.4.4. UTM Setup



Fig.4.5. Experiment with UTM



Fig.4.6. Experiment with Hardness Test Machine

## 8. Testing Results

In order to establish the composition gradient in the 5-6-layer transition zone, the feed rate of two powder feeders was controlled in this study. One feeder had powder made of the alloy Ti-6Al-4V, while the other included powder made of the alloy Co-Cr-Mo. It seems that the effect of temperature differences in the liquid metal pool as a result of compositional changes is directly responsible for the poor intermixing in the first two to three layers of the transition region that were deposited under the same conditions. Co-Cr-Mo alloy melts instantly by absorbing heat from the liquid metal pool inside the first layer of the transition area because it has a lower melting point than Ti-6Al-4V alloy (1604-1660 C). Because Co-Cr-Mo has a lower melting point than Ti-6Al-4V, this occurs.

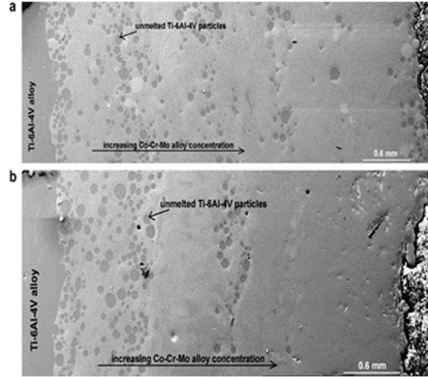


Fig.4.1 Typical microstructures of laser-processed Co-Cr-Mo graded coatings on Ti-6Al-4V alloy: (a) 50% Co-Cr-Mo alloy at the surface and (b) 86% Co-Cr-Mo alloy at the surface

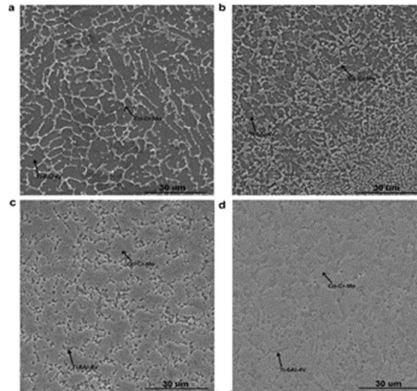
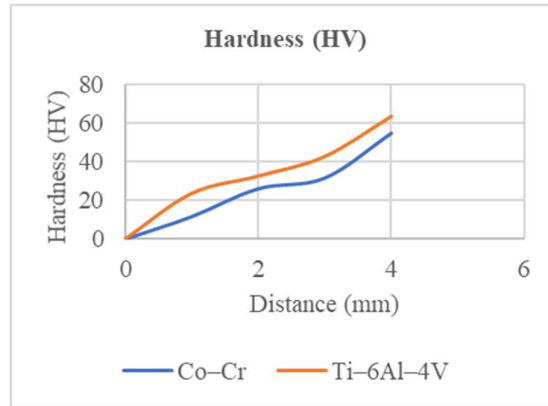


Fig.4.2 Top surface microstructures of gradient samples with varying concentration of Co-Cr-Mo alloy in top layer: (a) 25%, (b) 50%, (c) 70% and (d) 86%. The phase with the darker contrast is Ti-6Al-4V and that with the lighter contrast is Co-Cr-Mo alloy.

**Table.4.1 Hardness of Co-Cr & alloy structures**

Element	25%Coalloy	50%Coalloy	70%Coalloy	86%Coalloy
Ti	63.20	42.32	24.19	8.17
Al	5.79	3.29	3.58	4.22
V	3.64	2.35	2.75	1.74
Co	20.70	35.33	45.29	54.87
Cr	5.60	14.79	20.67	26.14
Hardness	588±27	670±28	789±38	947±22



Graph.4.1 Hardness variation across the gradient coatings

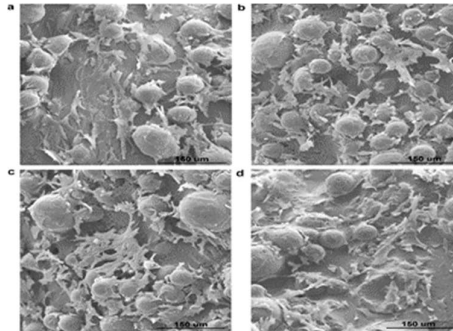
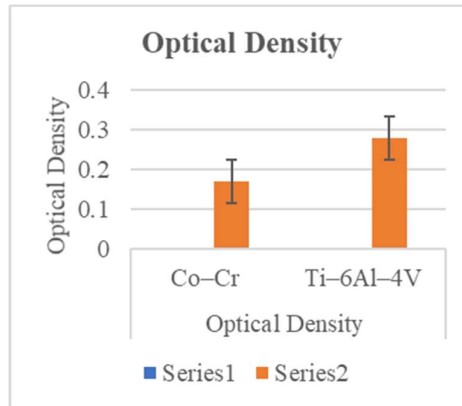


Fig.4.3 Culture on laser-processed gradient coatings with varying concentrations of Co-Cr alloy at the surface: (a) 100% Ti-6Al-4V alloy, (b) 25%, (c) 50%, (d) 70%, (e) 86% and (f) 100% Co-Cr alloy.



Graph.4.2 A higher optical density represents higher concentration of living cells.

Table.4.2 Properties of friction and wear testing materials

Work piece	Hardness	Roughness (Ra)	Density(g/cm <sup>3</sup> )
Un-Coated	382 HV	0.30	-
DLC coating	1750 HV	0.36	-
TiN coating	1950 HV	0.30	-
Cryogenic	401 HV	0.30	-
UHMWPE+ CNT 2 %wt	67.7 Shore D	0.20	0.94

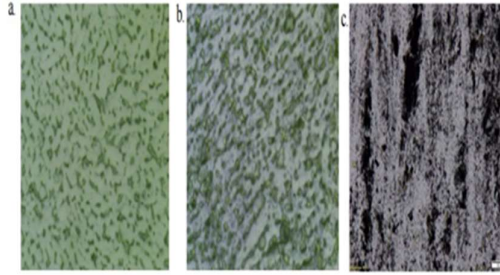
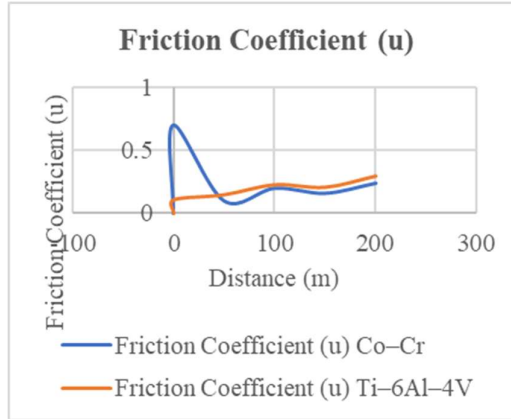
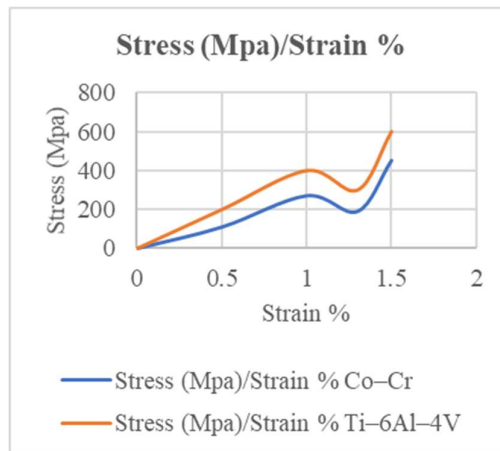


Fig.4.4 (a) Structure of Ti-6Al-4V; (b) Structure of 24 hr.-cryogenic treatment substrate Ti-6Al-4V (c) Dispersion of Carbon nanotube in UHMWPE



Graph.4.3 Friction coefficient versus sliding times for all experimental surface treatment Ti-6Al-4V pins against UHMWPE + 2% CNT disc

**Stress Strain Deflection Test Results**



Graph.4.4 Stress-strain curves and elastic modulus of the porous Ti6Al4V specimens with 30% porosity

**9. ANALYSIS**

It is self-evident that artificial components, known as prostheses, will need to be implanted into a human knee joint that has been rendered unusable either by the degenerative illness arthritis or by the trauma caused by an accident. The femur and the tibia are the two primary prosthesis that are utilized in complete knee replacement surgery. An artificial knee joint, also known as a femorotibial or tibiofemoral joint, is formed by the combination of these two prostheses. In order to operate properly under a variety of loading circumstances, the femorotibial joint has

to be flexed at a few distinct angles. Different biomaterials for the femur and the tibia at varying flexion degrees and sagittal radii under varying loading circumstances must be studied if the prosthetic joint is to work properly, wear among the femur and the tibia be reduced, and the life of the prosthetic joint be prolonged. . Other objectives of this study include extending the lifespan of prosthetic joints.

### Statistical Structural Analysis

#### 1. Geometry of knee cap model

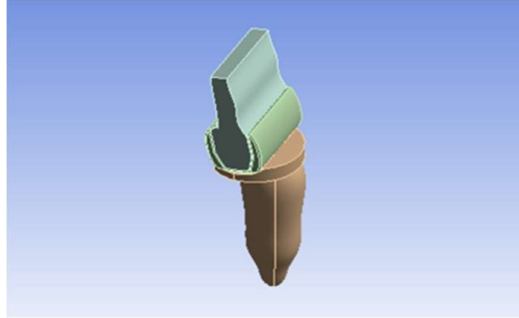


Fig.5.1 Geometry of knee cap model

Above figure shows Geometry of knee cap model of material ANSYS Software.

#### 2. Meshing of knee cap model

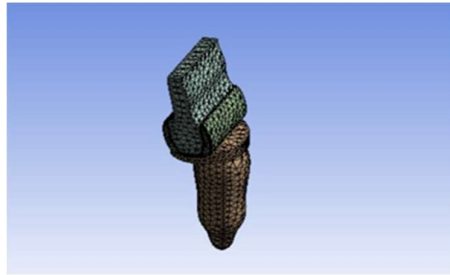


Fig.5.2 Meshing of knee cap model

Above figure shows Meshing of knee cap model of material ANSYS Software.

#### 3. Equivalent stress of knee cap model

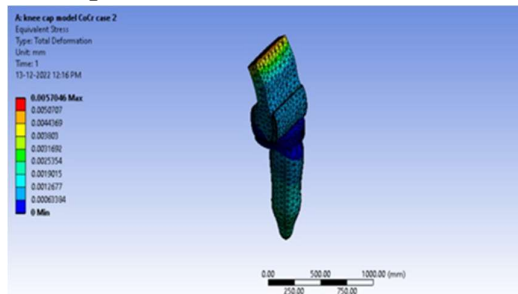


Fig.5.3 Equivalent stress of knee cap model

Above figure shows Equivalent stress of knee cap model of material is ANSYS Software Equivalent stress of knee cap model ranges between 0 MPa to 0.0057046 MPa.

#### 4. Equivalent Elastic strain of knee cap model

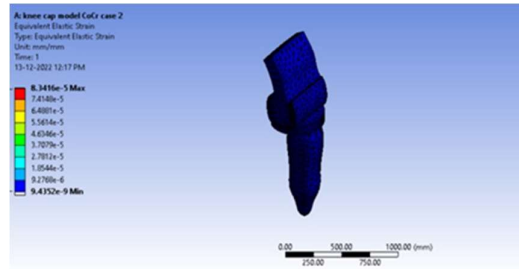


Fig.5.4 Equivalent Elastic strain of knee cap model

Above figure shows Equivalent Elastic strain of knee cap model of material is ANSYS Software Equivalent Elastic strain of knee cap model ranges between  $9.4352e-9$  Min to  $8.3416e-5$  max.

**5. Normal stress of knee cap model**

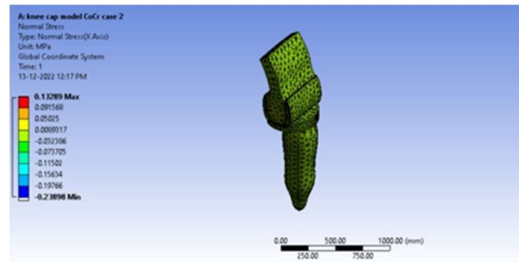


Fig.5.5 Normal stress of knee cap model

Above figure shows Normal stress of knee cap model of material is ANSYS Software Normal stress of knee cap model ranges between 0.13289 Max to -0.23898 Min.

**6. Total Deformation of knee cap model**

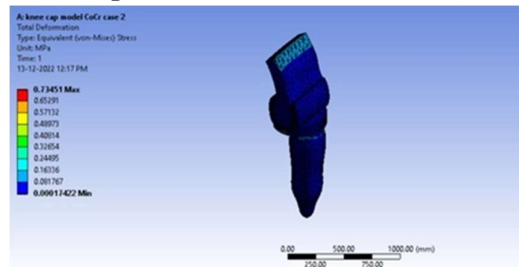


Fig.5.6 Total Deformation of knee cap model

Above figure shows Total Deformation of model of material is ANSYS Software Total Deformation of knee cap model ranges between 0.00017422 mm to 0.73451 mm.

**5.1. Contact Pressure of various materials**

Maximum contact stresses were determined between the chromium cobalt alloy, Ti-6Al-4V, and NiTi shape memory alloy femoral components and the polyethylene components and tibial cartilage. The data was tabulated and presented. The results for different materials were not statistically different, as shown by the available data. Maximum contact pressure was recorded after the menisci were removed and replaced with a flat plate of UHMWPE to increase reliability of the results. The size of this parameter, however, was discovered to be the same across all materials.

**1. Material CoCr**

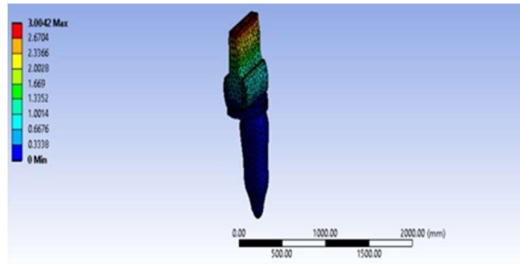


Fig.5.7 Contact pressure for material CoCr

Above figure shows Contact pressure for material CoCr of knee cap model. Contact pressure for material CoCr ranges between 0 mm to 3.1788 mm.

**2. Material Ti6Al4V**

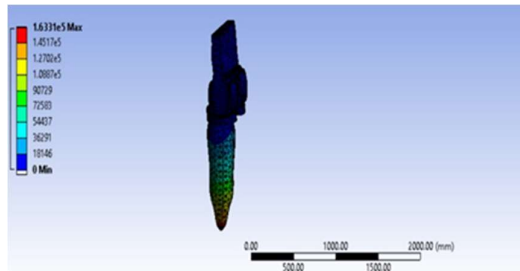


Fig.5.32 Contact pressure for material Ti6Al4V

Above figure shows Contact pressure for material Ti6Al4V of model. Contact pressure for material Ti6Al4V ranges between 0 mm to 1.6331e5 maxm.

**3. Material NiTi**

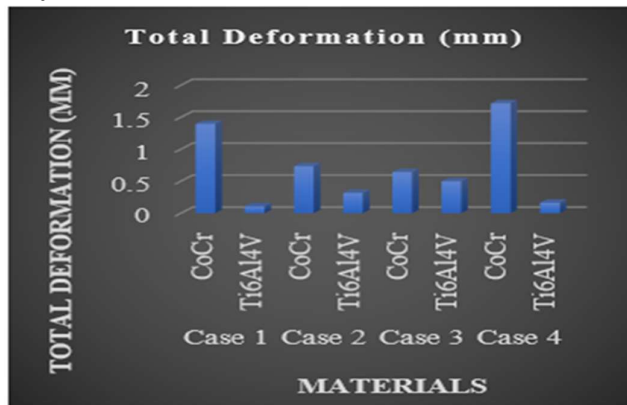
**Table.5.1 Contact pressure for various materials**

Materials	Contact Pressure on knee cap model (Mpa)
CoCr	3.17
Ti-6Al-4V	3.07

**10. ANALYTICAL RESULTS AND FINDINGS**

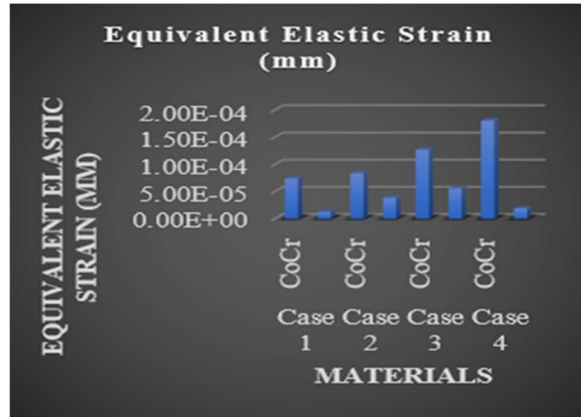
**10.1. Results for Case studies for Co-Cr & Ti6Al4V Materials**

**Static Structural Analysis**



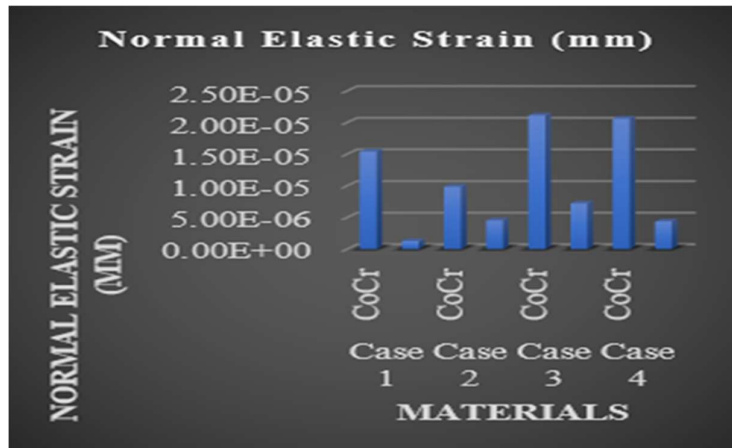
Graph.7.1 Total Deformation (mm)

As per the graph shows results of total deformation for materials CoCr and Ti6Al4V for case 1 case 2 & case 3, maximum deformation in case 4 for material CoCr and minimum deformation in case 1 for material Ti6Al4V.



**Graph.7.2 Equivalent Elastic Strain (mm)**

As per the graph shows results of Equivalent Elastic Strain for materials CoCr and Ti6Al4V for case 1 case 2 & case 3, maximum Equivalent Elastic Strain in case 4 for material CoCr and minimum Equivalent Elastic Strain in case 1 for material Ti6Al4V.



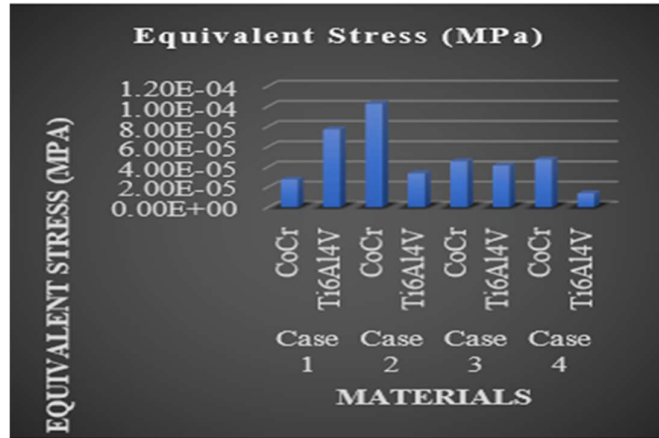
**Graph.7.3 Normal Elastic Strain (mm)**

As per the graph shows results of Normal Elastic Strain for materials CoCr and Ti6Al4V for case 1 case 2 & case 3, maximum Normal Elastic Strain in case 3 & 4 for material CoCr and minimum Normal Elastic Strain in case 1 for material Ti6Al4V.



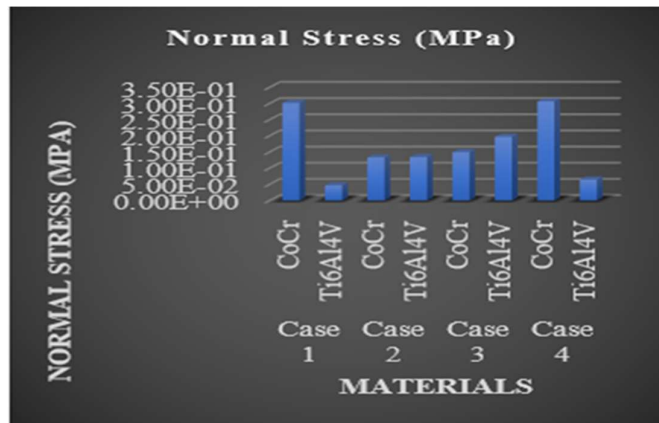
**Graph.7.4 Shear Elastic Strain (mm)**

As per the graph shows results of Shear Elastic Strain for materials CoCr and Ti6Al4V for case 1 case 2 & case 3, maximum Shear Elastic Strain in case 1 for material Ti6Al4V and minimum Shear Elastic Strain in case 1 for material CoCr and Ti6Al4V.



Graph.7.5 Equivalent Stress (MPa)

As per the graph shows results of Equivalent Stress for materials CoCr and Ti6Al4V for case 1 case 2 & case 3, maximum Equivalent Stress in case 2 for material CoCr and minimum Equivalent Stress in case 4 for material Ti6Al4V.F



Graph.7.6 Normal Stress (MPa)

As per the graph shows results of Normal Stress for materials CoCr and Ti6Al4V for case 1 case 2 & case 3, maximum Normal Stress in case 4 for material CoCr and minimum Normal Stress in case 1 for material Ti6Al4V.

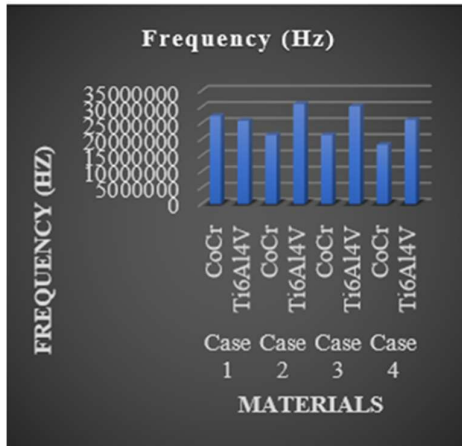


Graph.7.7 Shear Stress (MPa)

As per the graph shows results of Shear Stress for materials CoCr and Ti6Al4V for case 1 case 2 & case 3, maximum Shear Stress in case 1 for material CoCr and minimum Shear Stress in case 4 for material Ti6Al4V.

**Modal Analysis**

**1. For Natural Frequency**



Graph.7. 8 Frequency (Hz)

As per the graph shows results of Frequency for materials CoCr and Ti6Al4V for case 1 case 2 & case 3, maximum Frequency in case 2 for material Ti6Al4V and minimum Frequency in case 4 for material CoCr.

**2. For Total Deformation**

**1. Material CoCr**

**Total Deformation of knee cap model**

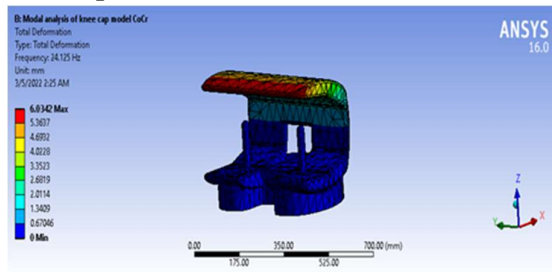


Fig.5.7 Total Deformation of knee cap model in modal analysis

Above figure shows Total Deformation of knee cap model of material CoCr Total Deformation of knee cap model ranges between 0 mm to 6.0342 mm.

**2. Material Ti6Al4V**

**Total Deformation of knee cap model**

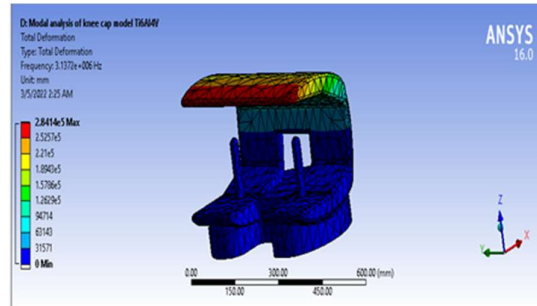


Fig.5.8 Total Deformation of knee cap model in modal analysis

Above figure shows Total Deformation of knee cap model of material Ti6Al4V. Total Deformation of knee cap model ranges between 0 mm to  $2.8414 \times 10^{-5}$  mm.

### 3. Material NiTi

#### Total Deformation of knee cap model

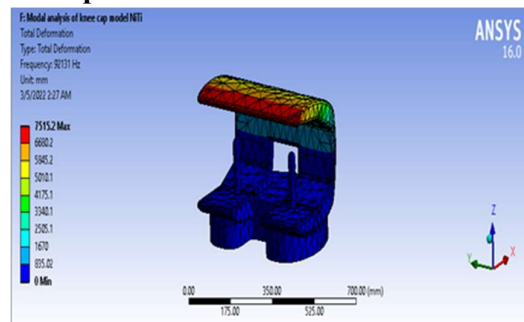


Fig.5.9 Total Deformation of knee cap model in modal analysis

Above figure shows Total Deformation of knee cap model of material Ni-Ti. Total Deformation of knee cap model ranges between 0 mm to 7515.2 mm.

According to analysis tools in modal analysis of Ansys and knee cap model in consideration, dynamic analysis are done. For this frequency and total deformation parameters are more than sufficient because if input frequency and natural frequency of the model gets matched than resonance occurs.

### 5.2. Comparative analysis of knee cap model with different materials

#### 1. Material CoCr

##### 1. Total Deformation of knee cap model

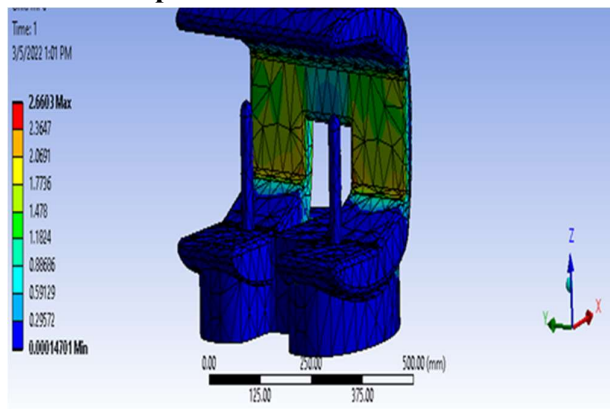


Fig.5.10 Total Deformation of knee cap model

Above figure shows Total Deformation of knee cap model of material CoCr Total Deformation of knee cap model ranges between 0.00014701 mm to 2.6603 mm.

**2. Equivalent stress of knee cap model**

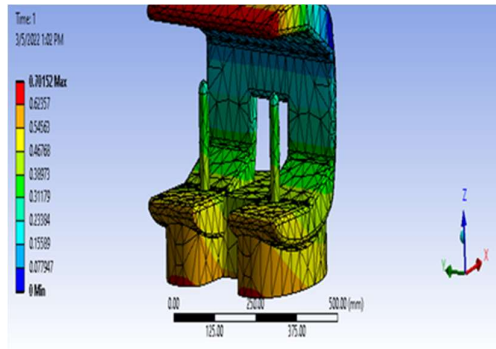


Fig.5.11 Equivalent stress of knee cap model

Above figure shows Equivalent stress of knee cap model of material CoCr Equivalent stress of knee cap model ranges between 0 mm to 0.70152 mm.

**3. Equivalent Elastic strain of knee cap model**

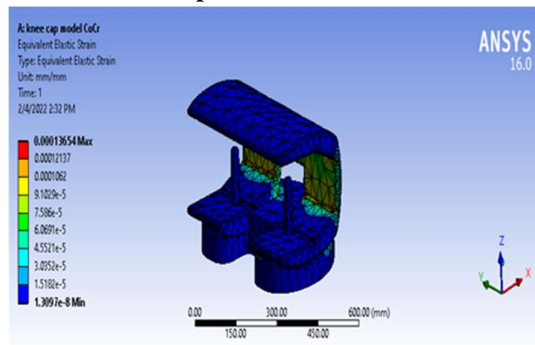


Fig.5.12 Equivalent Elastic strain of knee cap mode

Above figure shows Equivalent Elastic strain of knee cap model of material CoCr Equivalent Elastic strain of knee cap model ranges between 1.3097X 10 -8 to 0.00013654 mm.

**4. Normal stress of knee cap model**

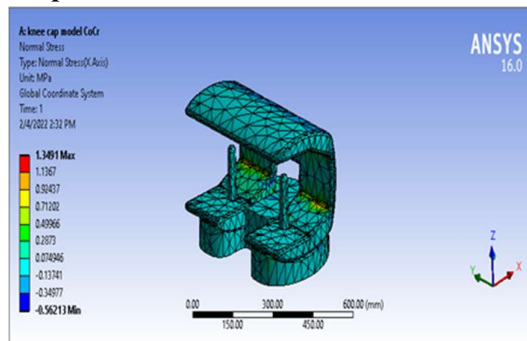


Fig.5.13 Normal stress of knee cap model

Above figure shows Normal stress of knee cap model of material CoCr Normal stress of knee cap model ranges between -0.56213 Mpa to 1.3491 Mpa.

**5. Shear stress of knee cap model**

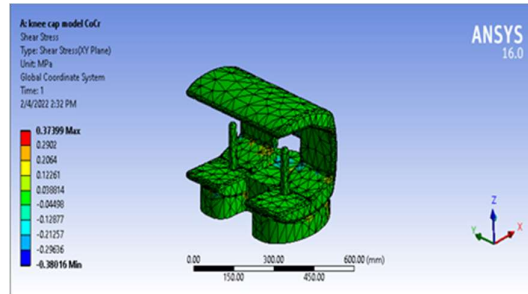


Fig.5.14 Shear stress of knee cap model

Above figure shows Shear stress of knee cap model of material CoCr Shear stress of knee cap model ranges between -0.38016 Mpa to 0.37399 Mpa.

**6. Normal Elastic strain of knee cap model**

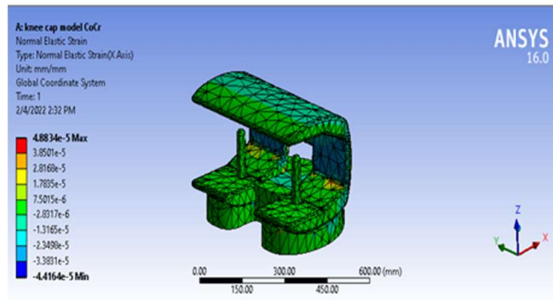


Fig.5.15 Normal Elastic strain of knee cap model

Above figure shows Normal Elastic strain of knee cap model of material CoCr Normal Elastic strain of knee cap model ranges between  $-4.4164 \times 10^{-5}$  to  $4.8834 \times 10^{-5}$  mm.

**7. Shear Elastic strain of knee cap model**

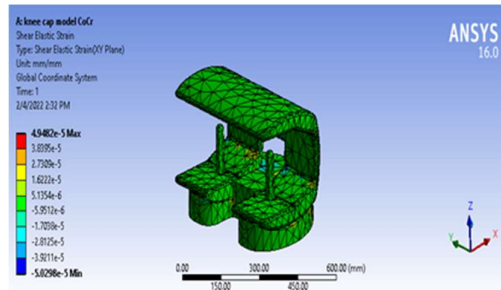


Fig.5.16 Shear Elastic strain of knee cap model

Above figure shows Shear Elastic strain of knee cap model of material CoCr Shear Elastic strain of knee cap model ranges between  $-5.0298 \times 10^{-5}$  to  $4.9482 \times 10^{-5}$  mm.

**2. Material Ni-Ti**

**1. Total Deformation of knee cap model**

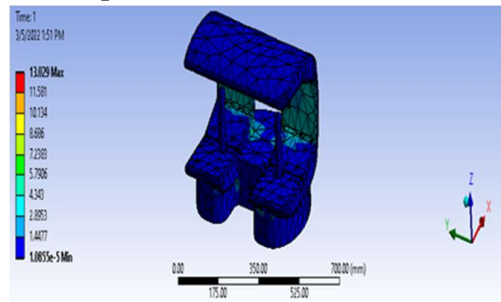


Fig.5.17 Total Deformation of knee cap model

Above figure shows Total Deformation of knee cap model of material Ni-Ti Total Deformation of knee cap model ranges between  $1.0855 \times 10^{-5}$  to 13.029mm.

**2. Equivalent stress of knee cap model**

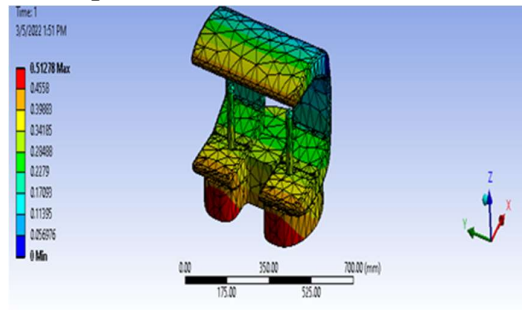


Fig.5.18 Equivalent stress of knee cap model

Above figure shows Equivalent stress of knee cap model of material Ni-Ti Equivalent stress of knee cap model ranges between 0 mm to 0.51278 mm.

**3. Equivalent Elastic strain of knee cap model**

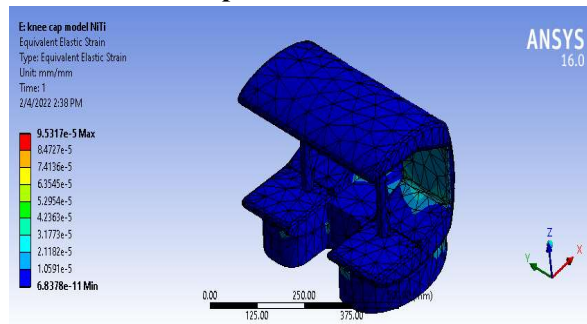


Fig.5.19 Equivalent Elastic strain of knee cap mode

Above figure shows Equivalent Elastic strain of knee cap model of material Ni-Ti Equivalent Elastic strain of knee cap model ranges between  $6.8378 \times 10^{-11}$  to  $9.5317 \times 10^{-5}$  mm.

**4. Normal stress of knee cap model**

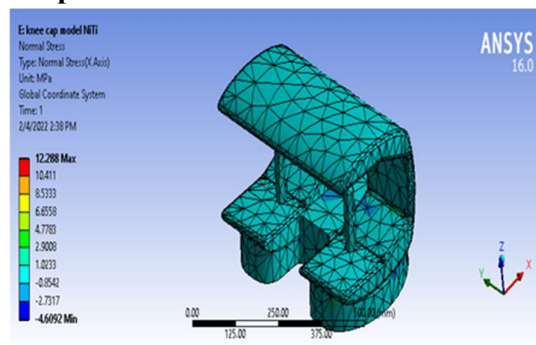


Fig.5.20 Normal stress of knee cap model

Above figure shows Normal stress of knee cap model of material Ni-Ti Normal stress of knee cap model ranges between -4.6092 Mpa to 12.288 Mpa.

**5. Shear stress of knee cap model**

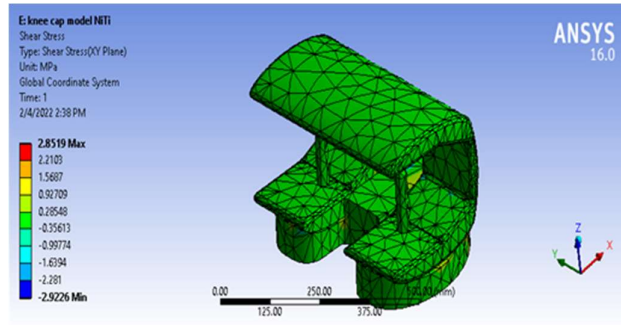


Fig.5.21 Shear stress of knee cap model

Above figure shows Shear stress of knee cap model of material Ni-Ti Shear stress of knee cap model ranges between -2.9226 Mpa to 2.8519 Mpa.

**6. Normal Elastic strain of knee cap model**

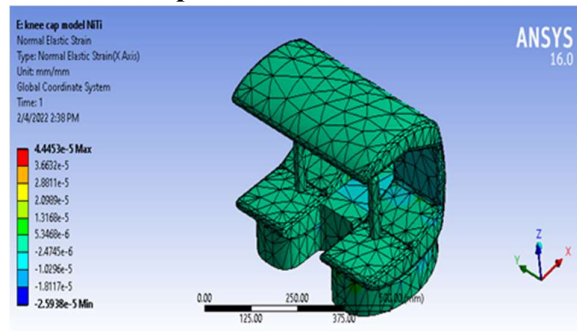


Fig.5.22 Normal Elastic strain of knee cap model

Above figure shows Normal Elastic strain of knee cap model of material Ni-Ti Normal Elastic strain of knee cap model ranges between -2.5938 X 10<sup>-5</sup> to 4.4453 X 10<sup>-5</sup> mm.

**7. Shear Elastic strain of knee cap model**

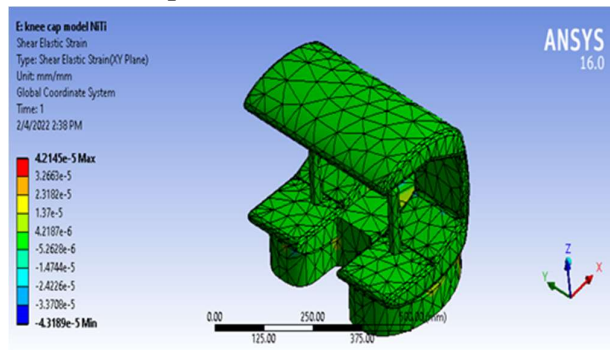


Fig.5.23 Shear Elastic strain of knee cap model

Above figure shows Shear Elastic strain of knee cap model of material Ni-Ti. Shear Elastic strain of knee cap model ranges between -4.3189 X 10<sup>-5</sup> to 4.2145 X 10<sup>-5</sup> mm.

**3. Material Ti-6Al-4V**

**1. Total Deformation of knee cap model**

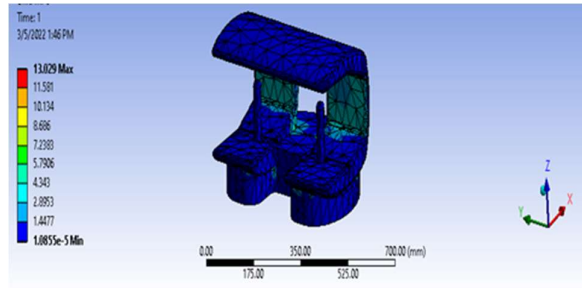


Fig.5.24 Total Deformation of knee cap model

Above figure shows Total Deformation of knee cap model of material Ti Total Deformation of knee cap model ranges between  $1.0855 \times 10^{-5}$  to 13.029 mm.

**2. Equivalent stress of knee cap model**

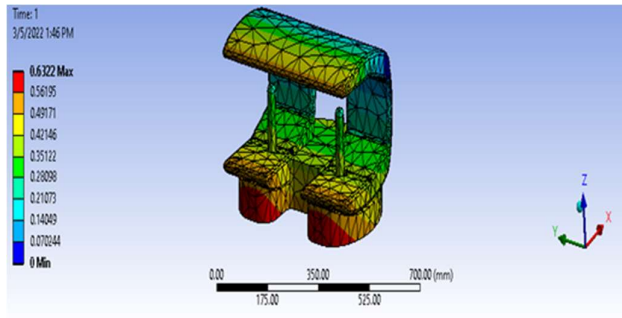


Fig.5.25 Equivalent stress of knee cap model

Above figure shows Equivalent stress of knee cap model of material Ti Equivalent stress of knee cap model ranges between 0 mm to 4.6322 mm.

**3. Equivalent Elastic strain of knee cap model**

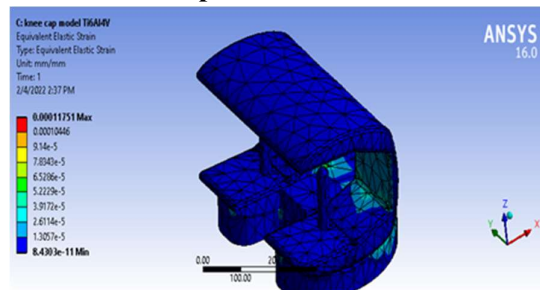


Fig.5.26 Equivalent Elastic strain of knee cap mode

Above figure shows Equivalent Elastic strain of knee cap model of material Ti Equivalent Elastic strain of knee cap model ranges between  $8.4303 \times 10^{-11}$  to 0.00011751 mm.

**4. Normal stress of knee cap model**

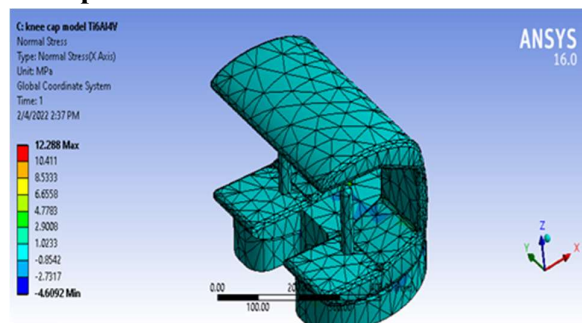


Fig.5.27 Normal stress of knee cap model

Above figure shows Normal stress of knee cap model of material Ti Normal stress of knee cap model ranges between  $-4.6092$  Mpa to  $12.288$  Mpa.

**5. Shear stress of knee cap model**

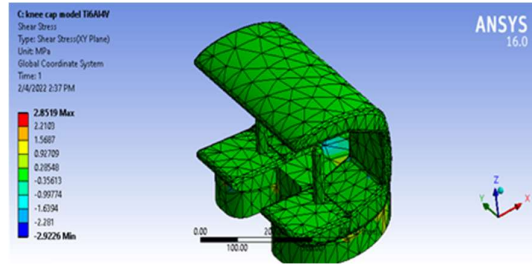


Fig.5.28 Shear stress of knee cap model

Above figure shows Shear stress of knee cap model of material Ti Shear stress of knee cap model ranges between  $-2.9226$  Mpa to  $2.8519$  Mpa.

**6. Normal Elastic strain of knee cap model**

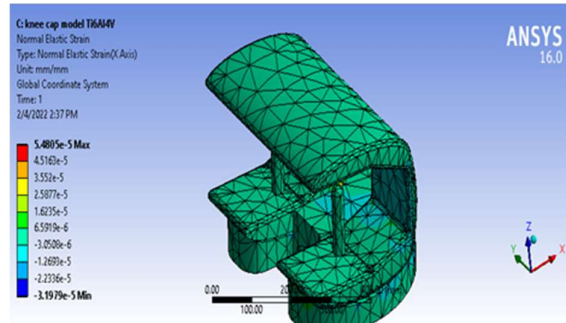


Fig.5.29 Normal Elastic strain of knee cap model

Above figure shows Normal Elastic strain of knee cap model of material Ti Normal Elastic strain of knee cap model ranges between  $-3.1979 \times 10^{-5}$  to  $5.4805 \times 10^{-5}$  mm.

**7. Shear Elastic strain of knee cap model**

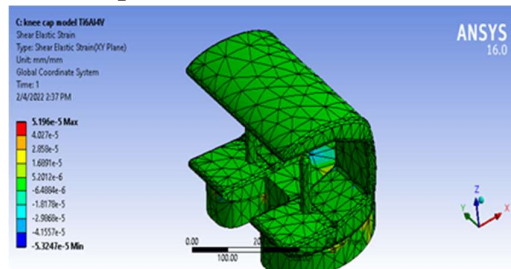


Fig.5.30 Shear Elastic strain of knee cap model

Above figure shows Shear Elastic strain of knee cap model of material Ti. Shear Elastic strain of knee cap model ranges between  $-5.3247 \times 10^{-5}$  to  $5.196 \times 10^{-5}$  mm.

**5.3. Contact Pressure of various materials**

Maximum contact stresses were measured on the polyethylene parts and also on the tibial cartilage when femoral part was chromium cobalt alloy, Ti-6Al-4V and NiTi shape memory alloy. The results were shown in table. It can be seen that there was no major difference in the results for different materials. For more confidence on the results, the menisci were replaced by a flat plate of UHMWPE and the maximum contact pressure was obtained on the plate, but it was found that the magnitude of this parameter was same for all the materials.

**1. Material CoCr**

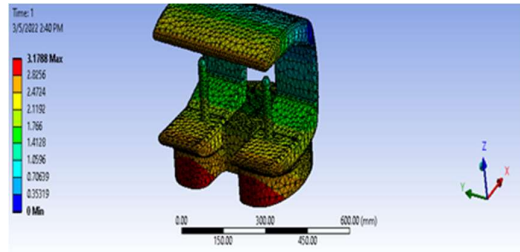


Fig.5.31 Contact pressure for material CoCr

Above figure shows Contact pressure for material CoCr of knee cap model. Contact pressure for material CoCr ranges between 0 mm to 3.1788 mm.

**2. Material Ti6Al4V**

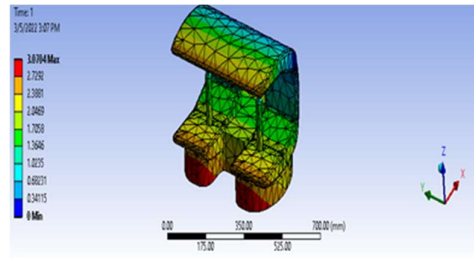


Fig.5.32 Contact pressure for material Ti6Al4V

Above figure shows Contact pressure for material Ti6Al4V of knee cap model. Contact pressure for material Ti6Al4V ranges between 0 mm to 3.0704 mm.

**3. Material NiTi**

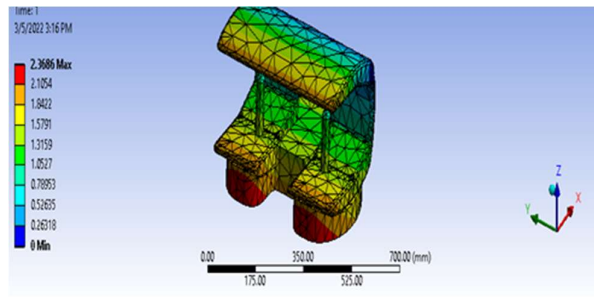


Fig.5.33 Contact pressure for material NiTi

Above figure shows Contact pressure for material NiTi of knee cap model. Contact pressure for material NiTi ranges between 0 mm to 2.3686 mm.

**Table.5.1 Contact pressure for various materials**

Materials	Contact Pressure on knee cap model (Mpa)
CoCr	3.17
Ti-6Al-4V	3.07

NiTi	2.36
------	------

## CONCLUSION AND FUTURE SCOPE

### Findings:

Comparative results of knee cap model with CoCr, NiTi and Ti6Al4V materials for 4 case studies

- According to the graph, which displays the findings of total deformation for materials CoCr and Ti6Al4V for cases 1, 2, and 3, the material CoCr experienced the most amount of distortion in case 4, while the material Ti6Al4V experienced the least amount of deformation in case 1.
- According to the graph, which displays the results of the equivalent elastic strain for the materials CoCr and Ti6Al4V for case 1, case 2, and case 3, the maximum equivalent elastic strain for the material CoCr was seen in case 4, while the minimum equivalent elastic strain for the material Ti6Al4V was seen in case 1.
- According to the data presented in the graph, which compares the Normal Elastic Strain of the materials CoCr and Ti6Al4V for cases 1, 2, and 3, the material CoCr exhibited the highest Normal Elastic Strain in cases 3 and 4, while the material Ti6Al4V exhibited the lowest Normal Elastic Strain in case 1.
- According to the graph, which displays the results of Shear Elastic Strain for materials CoCr and Ti6Al4V for cases 1, 2, and 3, the highest Shear Elastic Strain was observed in case 1 for the material Ti6Al4V, while the lowest Shear Elastic Strain was observed in case 1 for materials CoCr and Ti6Al4V.
- The results of the Equivalent Stress for the materials CoCr and Ti6Al4V are shown in the graph for cases 1, 2, and 3. The graph indicates that the greatest Equivalent Stress for the material CoCr occurs in case 2, while the least Equivalent Stress for the material Ti6Al4V occurs in case 4.
- According to the graph, which depicts the results of normal stress calculations for the materials CoCr and Ti6Al4V for cases 1, 2, and 3, the material CoCr experienced the highest normal stress in case 4, while the material Ti6Al4V experienced the lowest normal stress in case 1.
- According to the graph, which displays the findings of shear stress for the materials CoCr and Ti6Al4V for cases 1, 2, and 3, the material CoCr experienced the highest shear stress in case 1, while the material Ti6Al4V experienced the lowest shear stress in case 4.
- According to the graph, which displays findings of frequency for materials CoCr and Ti6Al4V for cases 1, 2, and 3, the highest frequency was seen for the material Ti6Al4V in case 2, while the lowest frequency was observed for the material CoCr in case 4.
- The knee cap model's total deformation, measured in millimetres, is shown above in the graph for the material Co-Cr used for the model. According to what we can observe, the Co-Cr material has a Total Deformation that runs anywhere from 0-350 mm.
- The graph that can be seen above displays the Total Deformation, measured in millimetres, of the knee cap model using Ti6Al4V as the material for the model.

According to what we can observe, the Total Deformation of the Co-Cr material spans from 0 to 450,000,000,000 millimetres.

- The graph that can be seen above displays the Total Deformation, measured in millimetres, of the knee cap model using Ti6Al4V as the material for the model. According to what we can observe, the Total Deformation of the Co-Cr material spans from 0 to 140,000 millimetres.
- The graph displays the total deformation in millimetres for four different cases and a specific material (NiTi) at a given time (1 second). The total deformation varies across the four cases, with Case 3 having the highest deformation (0.498 mm) followed by Case 2 (0.416 mm) and Case 4 (0.17369 mm), while Case 1 has the lowest deformation (0.1375 mm).
- The graph presents the values of equivalent elastic strain (measured in mm) for four different cases of NiTi alloy at a constant time interval of 1 second. The values of equivalent elastic strain increase as we move from Case 1 to Case 3, with the highest value recorded for Case 3. However, the value of equivalent elastic strain decreases in Case 4 as compared to Case 3. Overall, the table provides data on the elastic behavior of NiTi alloy under different loading conditions.
- The graph shows the normal elastic strain (in millimeters) for four different cases of NiTi (Nickel Titanium) at one second time interval. The strain values vary for each case, with Case 3 having the highest value of 7.28E-06 mm and Case 1 having the lowest value of 1.36E-06 mm. This data can be useful for understanding the elasticity properties of NiTi in different scenarios.

Comparative results of knee cap model with Co-Cr, Ti6Al4V and Ni-Ti materials

- The knee cap model's total deformation, measured in millimetres, is shown above in a graph along with the results for three distinct materials: Co-Cr, Ti6Al4V, and Ni-Ti. As can be seen, the Co-Cr material exhibits the largest Total Deformation, which may vary anywhere from 0 to 14 millimetres. After then, the Total Deformation of Ti6Al4V is lower than that of Co-Cr material, which may vary anywhere from 0-12mm. Ni-Ti also has the lowest Total Deformation value, which may vary anywhere from 0 to 4 mm.
- The above graph depicts the equivalent stress, measured in millimeters, that the knee cap model experiences for three distinct materials, namely Co-Cr, Ti6Al4V, and Ni-Ti. As can be seen, the material composed of Co-Cr has the largest equivalent stress, which may vary anywhere from 0 to 0.7mm. After then, the equivalent stress of Ti6Al4V is lower than that of the Co-Cr material, which varies from 0.0 to 0.65mm. Ni-Ti also has the lowest equivalent stress value, which may vary anywhere from 0 to 0.5mm.
- The above graph illustrates the equivalent elastic strain, measured in MPa, that the knee cap model experiences for three distinct materials, namely Co-Cr, Ti6Al4V, and Ni-Ti. According to what we have seen, the material composed of Co-Cr has the largest equivalent elastic strain, which is in the region of 0-0.00014MPa. After that, Ti6Al4V has a smaller equivalent elastic strain than the Co-Cr material, which has a range that is between 0 and 0.00012 MPa. Ni-Ti, on the other hand, has the lowest value of equivalent elastic strain, which varies from 0 to 0.0001 MPa.

- The above graph depicts the normal stress, measured in millimetres, that the knee cap model experiences for three distinct materials, namely Co-Cr, Ti6A14V, and Ni-Ti. As can be seen, the Co-Cr material exhibits the maximum normal stress, which falls anywhere between 0 and 13 millimetres. After then, the normal stress of Ti6A14V is lower than that of Co-Cr material, which may vary anywhere from 0-12mm. Ni-Ti also has the lowest normal stress value, which may vary anywhere from 0 to 2 mm.
- Shear stress in mm of knee cap model for three distinct materials, including Co-Cr, Ti6A14V, and Ni-Ti for the model may be seen in the graph that is located above. As can be seen, the Co-Cr material exhibits the largest shear stress, which falls anywhere between 0 and 2.5 millimetres. After then, the shear stress of Ti6A14V is lower than that of Co-Cr material, which may vary anywhere from 0-2.4mm. Ni-Ti also has the lowest shear stress value, which is between 0 and 0.5mm and fluctuates from there.
- The above graph illustrates the normal elastic strain, measured in MPa, of the knee cap model for three distinct materials, namely Co-Cr, Ti6A14V, and Ni-Ti, respectively. As can be seen, the normal elastic strain ranges for the Co-Cr material are between 0-6.5 x 10<sup>-5</sup> MPa, making it the material with the greatest normal elastic strain. After then, the typical elastic strain of Ti6A14V is lower than that of the Co-Cr material, which varies between 0-5.5X10<sup>-5</sup> MPa. And Ni-Ti has a typical elastic strain value that varies between 0-4.5X10<sup>-5</sup> MPa, making it the material with the lowest value.
- The shear elastic strain in MPa of the model knee cap is shown above on a graph for three distinct materials, including Co-Cr, Ti6A14V, and Ni-Ti, which are used for the model. As can be seen, the shear elastic strain ranges for the Co-Cr material are between 0-5.5 x 10<sup>-5</sup> MPa, making it the material with the greatest shear elastic strain. After then, the shear elastic strain of Ti6A14V is lower than that of Co-Cr material, which varies between 0 and 5 x 10<sup>-5</sup> MPa. And Ni-Ti has a shear elastic strain value that varies between 0-4.5X10<sup>-5</sup> MPa, making it the material with the lowest value.

### Conclusion

Using CATIA software, the design methodology for a tibial and femoral implant component has been developed in this study. A knee joint's static analysis has been performed using the ANSYS software by incorporating the contact pair between the components. In this investigation, static and modal analysis was performed on three distinct materials: Co-Cr, NiTi, and Ti6A14V. Also considered in this investigation were the four case studies and three distinct materials: Co-Cr, NiTi, and Ti6A14V.

To prevent permanent immobility in patients with arthritis or accident-related joint injury, a total knee prosthesis is required. According to the results of the analysis, decreasing the longitudinal radius of the TKR design decreases the shear tension, thereby reducing wear. As a result, the costs associated with enhancing knee joint treatments are reduced. In addition, the results indicate that NiTi material is stronger than ordinary polyethylene. In this Nickel titanium material, the total displacement is less than that of other materials. Therefore, NiTi is an effective material for Knee joint replacement.

The comparison of three materials, namely Co-Cr, Ti-6Al-4V, and TiNi, for prosthetic knee implants using a FEM approach revealed that each material has its unique advantages and disadvantages. Co-Cr is strong and wear-resistant but has poor biocompatibility and high natural frequencies. Ti-6Al-4V is biocompatible, strong, and corrosion-resistant, with lower

natural frequencies than Co-Cr, which reduces stress on the surrounding bone. TiNi has intermediate natural frequencies and has unique properties like super elasticity and shape memory. Cost-effectiveness analysis revealed that Nickel Titanium is the most cost-effective option, followed by Co-Cr and Ti-6Al-4V. Knee replacement surgery is an effective treatment for knee osteoarthritis and rheumatoid arthritis. The type of knee replacement surgery required depends on the severity of damage to the knee joint, and the most commonly used surgery is total knee replacement. The cost of surgery depends on several factors such as the type of implant used, the location of treatment, and the choice of orthopedic doctor and hospital.

Based on the objectives mentioned, it can be concluded that the study focused on analyzing the vibration behavior of prosthetic knee implants using the FEM approach. Different types of knee implants were studied, and the materials and methods used for various cases were analyzed using hospital patient data. The analysis of body mass patients was done to determine the appropriate combination of materials for obese individuals. The study implemented observational data in Ansys Workbench and conducted vibration analysis to evaluate the performance of the implants under consideration.

#### **Data Availability Statement**

The data that support the findings of this study are available from the corresponding author upon reasonable request. The data availability of all these Ansys work can be produced if demanded. The analysis in Ansys has 48 findings which cannot be described in single paper. Also the 4 cases of TKA taken from the hospital can also be produced if demanded.

#### **Future Scope**

- The analysis will be done for deep flexion angles.
- Thermal stresses at high temperature will be investigated.
- Different orientation of carbon fibers in polyethylene matrix will be considered.
- The results of analysis of femorotibial joint of a particular material combination will be verified by using a knee simulator.
- The theoretical method will be adopted to analyze the socket, but the design will lead to an increase in cost due to the increase in the safety factor.

#### **REFERENCES**

1. Abbas, E. N., Jweeg, M. J., & Al-Waily, M. (2020). Fatigue characterization of laminated composites used in prosthetic sockets manufacturing. *Journal of Mechanical Engineering Research and Developments*, 43(5), 384–399.
2. Abbas, S. M., Resan, K. K., Muhammad, A. K., & Al-Waily, M. (2018). Mechanical and fatigue behaviors of prosthetic for partial foot amputation with various composite materials types effect. *International Journal of Mechanical Engineering and Technology*, 9(9), 383–394.
3. Abbas, S. M., Sadiq, G. S. H., & Abdul Sattar, M. (2020). Improving the composite materials for Bi lateral prosthesis with below knee amputation. *Materials Science Forum*, 1002, 379–388. <https://doi.org/10.4028/www.scientific.net/MSF.1002.379>
4. Arami, A., Delaloye, J. R., Rouhani, H., Jolles, B. M., & Aminian, K. (2018). Knee Implant Loosening Detection: A Vibration Analysis Investigation. *Annals of Biomedical Engineering*, 46(1), 97–107. <https://doi.org/10.1007/s10439-017-1941-2>
5. Burn, E., Liddle, A. D., Hamilton, T. W., Judge, A., Pandit, H. G., Murray, D. W., & Pinedo-Villanueva, R. (2018). Cost-effectiveness of unicompartmental compared with

- total knee replacement: A population-based study using data from the National Joint Registry for England and Wales. *BMJ Open*, 8(4), 1–8. <https://doi.org/10.1136/bmjopen-2017-020977>
6. Cook, K., Forbes, S. P., Adamski, K., Ma, J. J., Chawla, A., & Garrison, L. P. (2020). Assessing the potential cost-effectiveness of a gene therapy for the treatment of hemophilia A. *Journal of Medical Economics*, 23(5), 501–512. <https://doi.org/10.1080/13696998.2020.1721508>
  7. Ferket, B. S., Feldman, Z., Zhou, J., Oei, E. H., Bierma-Zeinstra, S. M. A., & Mazumdar, M. (2017). Impact of total knee replacement practice: Cost effectiveness analysis of data from the Osteoarthritis Initiative. *BMJ (Online)*, 356, 1–12. <https://doi.org/10.1136/bmj.j1131>
  8. Hsu, C. Y., Tsai, Y. S., Yau, C. S., Shie, H. H., & Wu, C. M. (2019). Differences in gait and trunk movement between patients after ankle fracture and healthy subjects. *BioMedical Engineering Online*, 18(1), 1–13. <https://doi.org/10.1186/s12938-019-0644-3>
  9. Ibrahim, A., Yamomo, G., Willing, R., & Towfighian, S. (2021). Parametric study of a triboelectric transducer in total knee replacement application. *Journal of Intelligent Material Systems and Structures*, 32(1), 16–28. <https://doi.org/10.1177/1045389X20948581>
  10. Innocenti, B., Fekete, G., & Pianigiani, S. (2018). Biomechanical Analysis of Augments in Revision Total Knee Arthroplasty. *Journal of Biomechanical Engineering*, 140(11). <https://doi.org/10.1115/1.4040966>
  11. Kadhim, F. M., Chiad, J. S., & Enad, M. A. S. (2020). Evaluation and analysis of different types of prosthetic knee joint used by above knee amputee. *Defect and Diffusion Forum*, 398 DDF, 34–40. <https://doi.org/10.4028/www.scientific.net/DDF.398.34>
  12. Kamaruzaman, H., Kinghorn, P., & Oppong, R. (2017). Cost-effectiveness of surgical interventions for the management of osteoarthritis: a systematic review of the literature. *BMC Musculoskeletal Disorders*, 18(1), 1–17. <https://doi.org/10.1186/s12891-017-1540-2>
  13. Losina, E., Michl, G., Collins, J. E., Hunter, D. J., Jordan, J. M., Yelin, E., Paltiel, A. D., & Katz, J. N. (2016). Model-based evaluation of cost-effectiveness of nerve growth factor inhibitors in knee osteoarthritis: Impact of drug cost, toxicity, and means of administration. *Osteoarthritis and Cartilage*, 24(5), 776–785. <https://doi.org/10.1016/j.joca.2015.12.011>
  14. Mechi, S. A., & Al-Waily, M. (2021). Manufacturing and mechanical behavior investigation of prosthetic below knee socket by using natural kenaf fiber. *International Journal of Energy and Environment*, 12(1), Page45–62. [https://www.academia.edu/download/68799445/Prosthetic\\_Kenaf\\_Fiber\\_IJEE.pdf](https://www.academia.edu/download/68799445/Prosthetic_Kenaf_Fiber_IJEE.pdf)
  15. Takhakh, A. M., & Abbas, S. M. (2018). Manufacturing and analysis of carbon fiber knee ankle foot orthosis. *International Journal of Engineering and Technology(UAE)*, 7(4), 2236–2240. <https://doi.org/10.14419/ijet.v7i4.17315>
  16. Woiczinski, M., Steinbrück, A., Weber, P., Müller, P. E., Jansson, V., & Schröder, C. (2016). Development and validation of a weight-bearing finite element model for total

- knee replacement. *Computer Methods in Biomechanics and Biomedical Engineering*, 19(10), 1033–1045. <https://doi.org/10.1080/10255842.2015.1089534>
17. Yousif, L. E., Resan, K. K., & Fenjan, R. M. (2018). Temperature effect on mechanical characteristics of a new design prosthetic foot. *International Journal of Mechanical Engineering and Technology*, 9(13), 1431–1447.